Optics and Spectroscopy, 2023, Vol. 131, No. 6

02

Raman scattering spectroscopy to estimate surface of VT6 titanium alloys

© P.E. Timchenko[1,2], O.O. Frolov[1,2], E.V. Timchenko[1,2,¶], D.A. Dolgushkin[2], A.N. Nikolaenko[2], L.T. Volova[2], V.V. Ivanov[2], R.T. Samigullin[1]

[1] Samara University, Samara, Russia
[2]Samara State Medical University, „BioTech", biotechnology center, 443079 Samara, Russia
[¶]e-mail: laser-optics.timchenko@mail.ru

Received October 28, 2023
Revised November 23, 2022
Accepted November 28, 2022

The results of Raman scattering spectroscopy studies of the surface of implant samples with different types of coatings are presented. Samples based on the VT6 titanium alloy manufactured by the selective laser sintering technique with different coatings (without coatings, with a calcium hydroxyapatite coating, with a combined coating of calcium hydroxyapatite with an antimicrobial drug coating applied on top, and samples with a chitosan-containing coating) were studied. Spectral differences between surfaces of VT6 titanium-based implant samples with different types of coatings are found. The findings will allow studying the dynamics of resorption of these coatings by Raman scattering spectroscopy in preclinical studies in animals.

Keywords: Raman scattering spectroscopy, surface, titanium alloy, scanning electron microscopy.

DOI: 10.61011/EOS.2023.06.56654.101-23

Introduction

Improvement of metal fixatives is one of main challenges in the modern reconstructive surgery. Apart from strength properties, an increasingly greater attention is paid to biointegrative properties of implants that define to a significant extent the efficiency of surgical operation, the duration of implant functioning, the patient quality of life [1–3].

Improvement of implant coatings, in particular those of endografts, is a pressing challenge in traumatology and orthopedics. The frequency of revision surgery following endoprosthesis replacement of large joints is as high as up to 20% of primary surgical operations. This is related to both the mechanical wear of the device, traumatization and the development of complications — aseptic and septic instability of endoprosthesis components. In 2.5% of primary endoprosthesis replacement of hip and knee joints cases and in 10% of revision endoprosthesis surgical operation periprosthetic joint infection may occur [4,5].

Surface properties of the implants often play a critical role in bacteria adhesion followed by a biofilm formation on the implant. The development of a titanium implant coating preventing such complications is of interest [6,7].

Researchers all over the world are trying to develop different types of coatings for orthopedic implants. Coatings based on chitosan, hydroxyapatite, biocoatings containing antimicrobal drugs, combined coatings are developed [8,9]. One of the main challenges remains duration of bioactivity of any coating, its interaction with human organism. Some coatings imply gradual release of the active medicinal drug from them, further resorption of the top coating, and manifestation of the biological effect lower coatings of the implant [10,11].

Currently, physical research methods have found wide application for biomedical purposes [12–14]. One of methods to evaluate properties of implant surfaces with different types of coatings can be the Raman scattering spectroscopy (RSS), which is a noninvasive and commonly used method in healthcare [15].

The goal of this study was to comparatively evaluate surface properties of implant samples based on VT6 titanium with different types of coatings using Raman scattering spectroscopy and scanning electron microscopy.

Materials and research methods

The studied materials were implant samples based on VT6 titanium manufactured by selective laser sintering (Pavlov University). The samples under study are split into 4 groups: I — sterile samples (without coatings), II — samples with calcium hydroxyapatite (HAp) coating (National Research Tomsk Polytechnic University), III — samples with calcium hydroxyapatite coating with additionally applied antimicrobial drug coating (Skolkovo Institute of Science and Technology), IV — samples with coating with chitosan containing film (Lomonosov Moscow State University, Department of Polymer and Crystal Physics). All samples were sterilized by standard methods used in healthcare clinics.

The samples of VT6 titanium with coating produced for the RSS study are cylinder bars with a length of 5 mm and a diameter of 2 mm.

The sample surfaces were pre-evaluated by scanning electron microscopy using a JED-2300 scanning electron microscope (by TokyoBoeki, Japan) with AnalysisStation

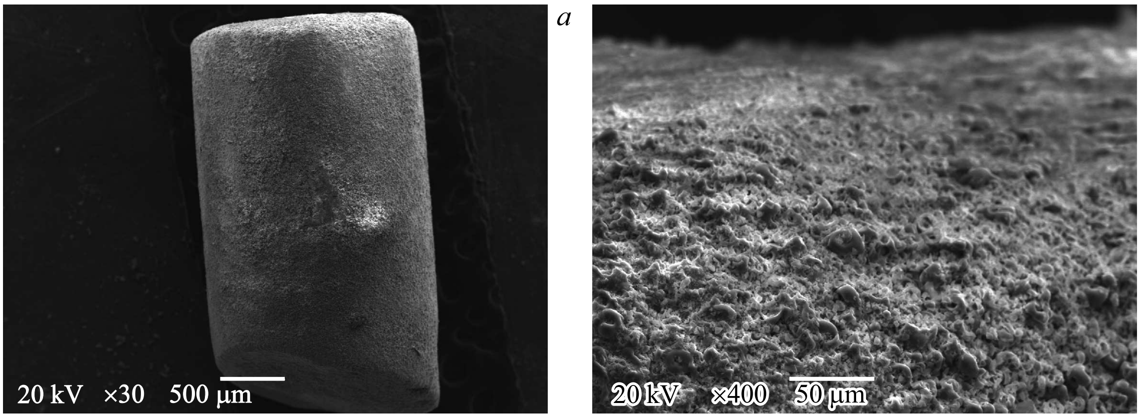

Figure 1. Scanning electron microscopy of a VT6 titanium sample with hydroxyapatite coating. *a* — 30x magnification, *b* — 400x magnification.

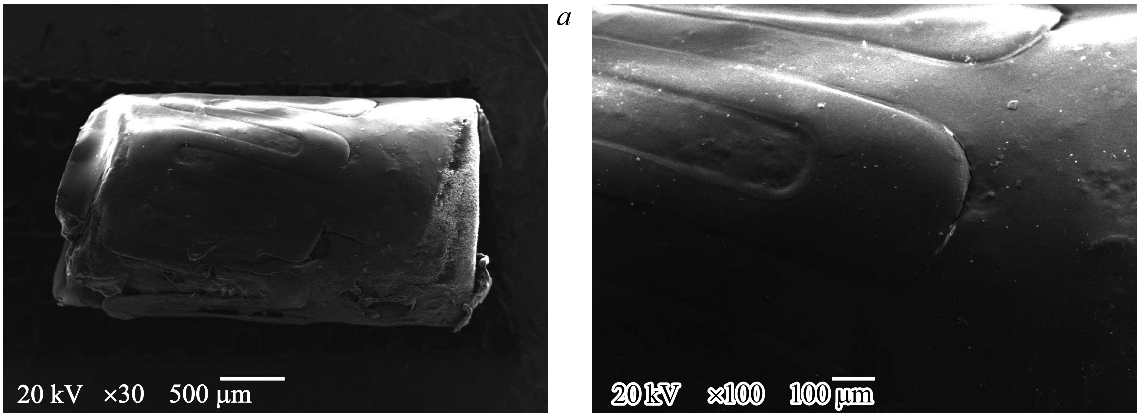

Figure 2. Scanning electron microscopy of a VT6 titanium sample with a combined coating of hydroxyapatite and an antimicrobal drug applied on top of it: *a* — 30x magnification, *b* — 100x magnification.

3.63.01 software. Coating have been sputtered using a EMITECHK450X unit (Great Britain).

Studies were conducted *in vivo* by the method of Raman scattering spectroscopy, which was implemented using a bench composed of a semiconductor laser (LML-785.0RB-04), an optical module of Raman scattering (PBL 785), a spectrograph (Sharmrock SR-303i) with an integrated digital camera (ANDOR DV-420A-OE) cooled to -60°C, and a computer [16].

The use of this spectrograph provided a wavelength resolution of 0.15 nm at a low level of inherent noise. The laser emission power of 400 mW within the exposure times used (30 s) did not caused changes in the samples. RS spectra were recorded using an optical probe placed above the subject under study at a distance of 7 mm. In this study the RS spectra were analyzed in the range of $400-1800\,\mathrm{cm}^{-1}$.

To exclude the autofluorescence contribution in the RS spectrum, the method of subtraction of the fluorescent component of polynomial approximation was used with additional filtration of random noise effects. The RS spectra were processed and analyzed using Wolfram Mathematica 12.2 software package [17].

Results

The study of sample surfaces by scanning electron microscopy has revealed differences between them. Thus, the VT6 titanium samples with hydroxyapatite sputtered on them were characterized by a uniform distribution of coating over the implant surface area. No uncoated areas, coating lesions or bevels, including those on the bases of cylindrical samples, have been found with different magnifications. It can be seen with the 400x magnification, that the coating is rough and microporous, which fact should be taken into account when performing the RSS (Fig. 1).

The following should be noted from the visual analysis of electron microscopy of VT6 titanium samples with the combined coating, i.e. hydroxyapatite with antimicrobal drug applied on top of it. The antimicrobal coating is applied on the sample unevenly. Conspicuous are the sample areas without the top layer and coated with

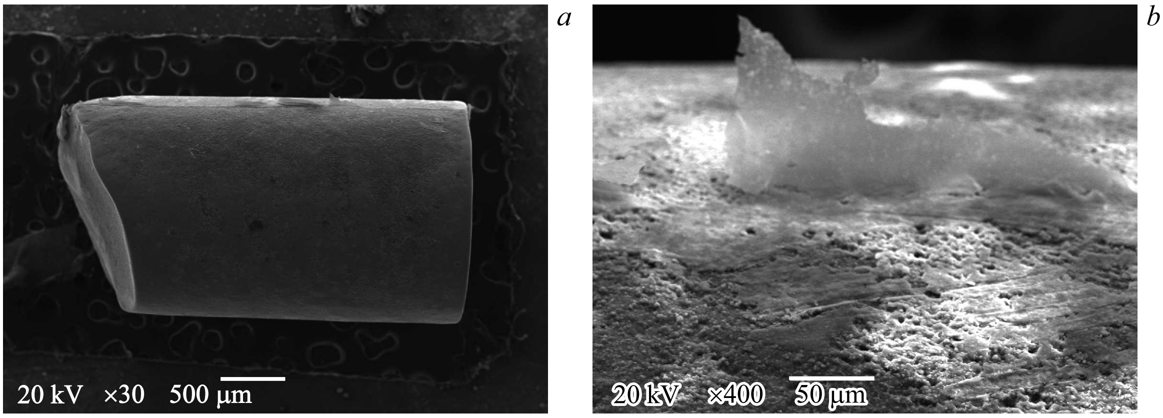

Figure 3. Scanning electron microscopy of a VT6 titanium sample with chitosan coating: *a* — 30x magnification, *b* — 400x magnification.

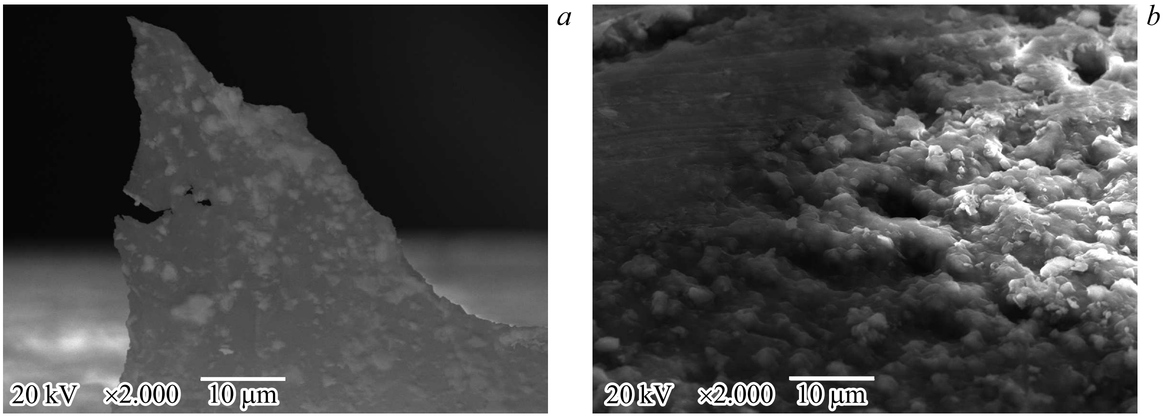

Figure 4. Scanning electron microscopy of a VT6 titanium sample with chitosan coating, 2000 magnification: *a* — particles of the coating on peeling off elements; *b* — particles of the coating on the implant surface.

hydroxyapatite only (Fig. 2, *a*). The top antimicrobal layer is nonuniform: there is a clearly seen spiral-form area over its entire surface separated by a deepened groove (Fig. 2, *b*).

Visual examination of VT6 titanium samples with chitosan coating has revealed elements of the coating peeled off in the form of dry scales. A similar pattern was observed with electron microscopy of samples at low magnifications (Fig. 3, *a*). These fragments were easily separable by forceps, laid freely in a sterile package.

However, with the high-magnification electron microscopy study it has been found that both the peeling off areas and the surface of the entire sample were evenly coated with whitish impregnations of different shapes and sizes (Fig. 3, *b*, Fig. 4). This fact suggested that the presence of peeling off scales should not be interpreted as a defect of coating. Accordingly, the RSS study of these samples should be conducted also with aim to find out element structures similar to the chitosan structure.

The Raman scattering spectroscopy study of sample surfaces has revealed the following features.

Fig. 6 shows normalized Raman scattering spectra of the samples under study. The interpretation of main spectral lines is presented in the table.

As can be seen from Fig. 5, RS spectra have clearly defined spectral differences between the spectra of all groups under study.

The differences between group 4 (samples coated with a chitosan-containing film) and group 1 (sterile samples) are manifested on RS lines $\sim 1260\,\mathrm{cm}^{-1}$ (Amide III-Dueto C–N stretchingand N–H bending), $\sim 1416\,\mathrm{cm}^{-1}$ (CH deformation), $\sim 1558\,\mathrm{cm}^{-1}$ (Amide II Parallel/Antiparallel β-sheet structure), $\sim 1665\,\mathrm{cm}^{-1}$ (Amide I vibration) and $1748\,\mathrm{cm}^{-1}$ (ν(C=O estergroup), phospholipids (Lipid assignment)).

The above-specified RS lines $\sim 1260\,\mathrm{cm}^{-1}$, $\sim 1416\,\mathrm{cm}^{-1}$, $\sim 1558\,\mathrm{cm}^{-1}$, $\sim 1665\,\mathrm{cm}^{-1}$, $1748\,\mathrm{cm}^{-1}$ are not manifested in sample group 2 (samples with HAp coating), however, the lines are clearly manifested in the range of $950-1050\,\mathrm{cm}^{-1}$ that contains lines of hydroxyapatite $955-961\,\mathrm{cm}^{-1}$ (PO_4^{3-} (ν_1) (P–O symmetric stretch)) and $\sim 432\,\mathrm{cm}^{-1}$ (PO_4^{3-} (ν_2) (P–O symmetric stretch) (phosphate of HA)).

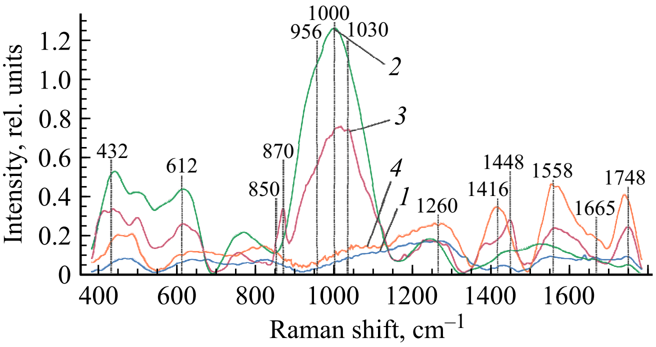

Figure 5. Averaged RS spectra of VT6 titanium alloy samples under study. *1* — VT6 titanium without coating (reference), *2* — HAp coating, *3* — HAp coating with antibiotic drug, *4* — coating with chitosan.

In group 3 (samples with HAp coating and antimicrobal drug) the lines in the range of 950–1050 cm^{-1} are less manifested as compared to sample group 2, there are RS lines of $\sim$ 1260 cm^{-1}, $\sim$ 1448 cm^{-1}, $\sim$ 1558 cm^{-1}, $\sim$ 1665 cm^{-1}, 1748 cm^{-1}. Group 3 has a clearly manifested RS line of KP 870 cm^{-1} ν(C–C), Benzene ring of hydroxylproline (collagen assignment), which is related to the presence of antimicrobal drug in the film.

To increase the informative value of obtained RS spectra, a nonlinear regression analysis of the spectra was carried out, consisting in decomposition into spectral lines.

The composition of spectral lines is determined on the basis of automatic multi-iteration modeling of 48 RS spectra in the Wolfram Mathematica 12.2 software system using machine learning methods and approved by results of literature analysis (see the table). When modeling the profile of the spectral lines used as a template, the position of x_0 and the half width at half-maximum (HWHM) dx of a line were fixed non-rigidly.

When modeling, only the line intensity was fit in the range from 0 to the local maximum of the spectrum near x_0. The HWHM was limited in the range from 1 to 16 cm^{-1}. This allowed achievement of high stability of the results when modeling the profile and taking into consideration all shifts of RS lines.

The criterion variable was the amplitude of lines a, which is dependent on the independent regressors dx and x_0 that determine initial conditions of the analysis. The average corrected coefficient of determination for the initial spectrum in the range of 400–1800 cm^{-1} for all 60 spectra was ${}_{\text{adj}}R^2 = 0.998$.

The normalized amplitudes of the decomposed Raman lines were used for the relative quantitative analysis of the component composition. The obtained data was analyzed in the Wolfram Mathematica 12.2 software system using the method of logistic regression.

The results of the classification using the method of logistic regression in reduced two-dimensional measurements are shown in Fig. 6 as a probability density distribution of each

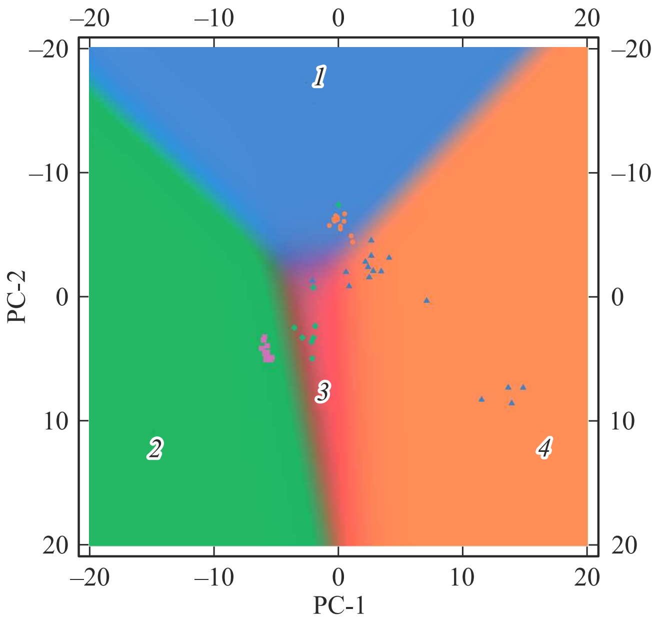

Figure 6. 2D distribution of probability of each class as a function of attributes (samples: *1* — VT6 titanium without coating (reference), *2* — HAp coating, *3* — HAp coating with antibiotic drug, *4* — coating with chitosan).

measurement classified as one of the four studied classes. It can be seen that the areas of groups are well differentiated and have no significant intersections.

As a result of the analysis by the method of logistic regression, a discriminant model of characteristic changes in intensities of RS lines for VT6 titanium samples with different coatings is formed. The calculated accuracy was = 100%, the base line accuracy was = 33.7% (classification between the closest classes). The discriminant adequacy of the method is characterized by the value of AUC = 1. The decision matrix of the model to classify the studied samples is shown in Fig. 7.

Fig. 8, *a* shows results of LDA comparison of sample groups. Discriminant function LD-1 describes 73.4% dispersion. Positive values of LD-1 are typical for RS spectra of samples with HAp coating. Areas of the groups have no intersections.

Fig. 8, *b* shows coefficients of the factor structure matrix for the most significant RS lines with a physical meaning of correlation between the variables in the model and the discriminant function.

The higher is LD-1 value modulus for a variable, the greater is significance of this variable in determining the difference in the discrimination model between groups of samples. For example, spectra with HAp have higher relative intensity of the RS line 956 cm^{-1} , which is reflected by a positive value of 0.61 of the $k956$ coefficient of the factor structure. $k1260$, $k1416$, $k1665$ coefficients are higher for samples with chitosan coating. The percentage of correctly classified values at cross-validation was 93.8%.

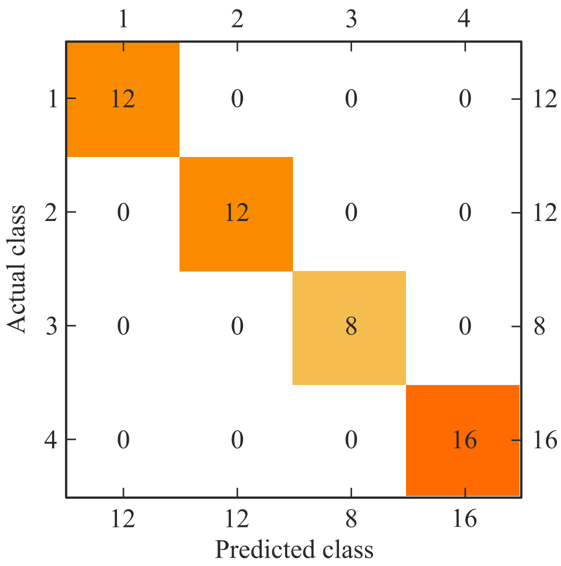

Figure 7. Decision matrix of the model to classify the studied samples (samples: *1* — VT6 titanium without coating (reference), *2* — HAp coating, *3* — HAp coating with antibiotic drug, *4* — coating with chitosan).

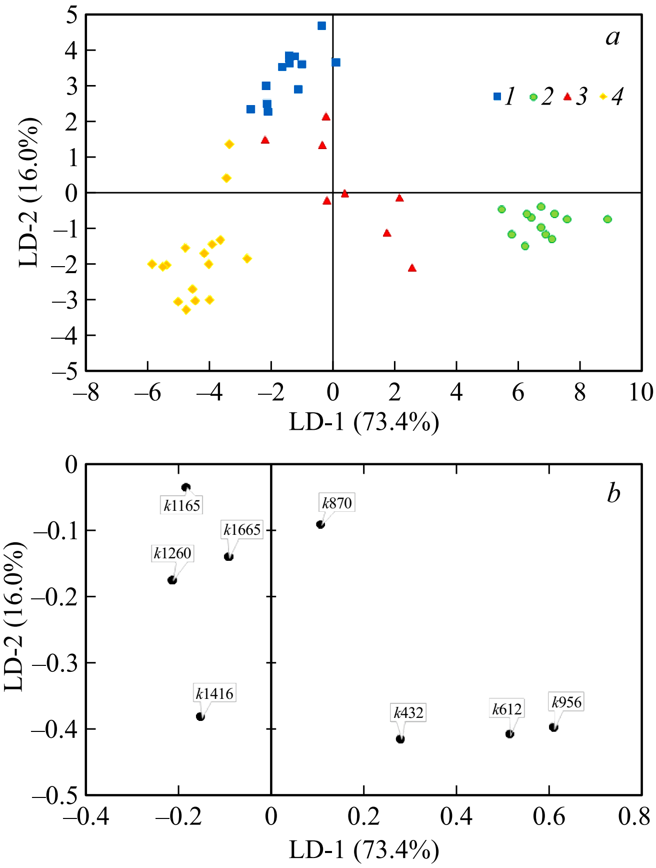

Figure 8. LDA results: *a* — linear discriminant function curve (samples: *1* — VT6 titanium without coating (reference), *2* — HAp coating, *3* — HAp coating with antibiotic drug, *4* — coating with chitosan); *b* — values of factor structure coefficients.

Conclusions

The study of sample surface by scanning electron microscopy allowed revealing features of coating application on samples, revealing defects, features of relief or, in contrast, suggesting uniform application of the coating over the implant surface. In accordance with this, the scheme of RSS study of samples should be planned and results of the procedure should be interpreted.

As a result of surface RSS of VT6 titanium samples with different types of coatings the spectral differences has been found between studied groups using the processing of results by the method of logistics regression and LDA statistical analysis.

Main spectral differences between group 4 (samples coated with a chitosan-containing film) and group 1 (sterile samples) are manifested on the following lines: $\sim 1260\,\mathrm{cm^{-1}}$ (Amide III), $\sim 1416\,\mathrm{cm^{-1}}$ (CH deformation), $\sim 1558\,\mathrm{cm^{-1}}$ (Amide II), $\sim 1665\,\mathrm{cm^{-1}}$ (Amide I) and $1748\,\mathrm{cm^{-1}}$ (phospholipids).

The above-specified RS lines of $\sim 1260\,\mathrm{cm^{-1}}$, $\sim 1416\,\mathrm{cm^{-1}}$, $\sim 1558\,\mathrm{cm^{-1}}$, $\sim 1665\,\mathrm{cm^{-1}}$, $1748\,\mathrm{cm^{-1}}$ are not manifested in sample group 2 (samples with HAp coating), however, the results show clearly distinguished lines in the range of $950-1050\,\mathrm{cm^{-1}}$ corresponding to hydroxyapatite lines of $955-961\,\mathrm{cm^{-1}}$ ($PO_4^{3-}(\nu_1)$) and $432\,\mathrm{cm^{-1}}$ ($PO_4^{3-}(\nu_2)$). In group 3 (samples with HAp and antimicrobal drug coating) the RS intensity in the range of $950-1050\,\mathrm{cm^{-1}}$ was less manifested as compared to sample group 2 (samples with HAp coating), and RS lines of $\sim 1260\,\mathrm{cm^{-1}}$, $\sim 1448\,\mathrm{cm^{-1}}$, $\sim 1558\,\mathrm{cm^{-1}}$, $\sim 1665\,\mathrm{cm^{-1}}$, $1748\,\mathrm{cm^{-1}}$ were present. In this group a clearly manifested RS line of $870\,\mathrm{cm^{-1}}$ (Benzenering of hydroxyproline) was observed.

As a result of the conducted study main spectral characteristics and their differences has been established for surfaces of implant samples with different types of coatings based on VT6 titanium. In further pre-clinical studies in animals, it is planned to implant these samples with their following removal to evaluate surface changes in dynamics. The knowledge of spectral characteristics of implant surfaces will help in establishing the laws of coatings resorption, in proving or disproving their biological effect in the pre-clinical study dynamics.

Conflict of interest

The authors declare that they have no conflict of interest.

References

[1] G. Pellegrini, L. Francetti, B. Barbaro, M. Del Fabbro. J. Investig. Clin. Dent., **9** (4), e12349 (2018).
DOI: 10.1111/jicd.12349

[2] MQ. Chen. Front. Bioeng. Biotechnol., **10**, 878257 (2022). DOI: 10.3389/fbioe.2022.878257
[3] M.M. Saleh, A.H. Touny, M.A. Al-Omair, M.M. Saleh. Biomed. Mater. Eng., **27** (1), 87–99 (2016) DOI: 10.3233/BME-161568. PMID: 27175470
[4] W. Zimmerli, P. Sendi. APMIS, **125** (4), 353–364 (2017) DOI: 10.1111/apm.12687
[5] E.A. Baker, M.M. Fleischer, A.D. Vara, M.R. Salisbury, K.C. Baker, P.T. Fortin, C.R. Friedrich. Nanomaterials, **11** (3), 583 (2021). DOI: 10.3390/nano11030583
[6] D. Losic. Expert Opin. Drug Deliv., **18** (10), 1355–1378 (2021). DOI: 10.1080/17425247.2021.1928071
[7] S. Maher, A. Mazinani, M.R. Barati, D. Losic. Expert Opin. Drug Deliv., **15** (10), 1021–1037 (2018). DOI: 10.1080/17425247.2018.1517743.
[8] S. Kumari, H.R. Tiyyagura, Y.B. Pottathara, K.K. Sadasivuni, D. Ponnamma, T. Douglas, A.G. Skirtach, M.K. Mohan. Carbohydrate Polymers, **255**, 117487 (2021). DOI: 10.1016/j.carbpol.2020.117487
[9] A.A. Vu, S. Bose. ACS Appl. Mater. Interfaces., **12** (47), 52383–52392 (2020). DOI: 10.1021/acsami.0c14993
[10] C.L. Roman., H. Tsuchiya, I. Morelli, A.G. Battaglia, L. Drago. Bone Joint Res., **8** (5), 199–206 (2019). DOI: 10.1302/2046-3758.85.BJR-2018-0316
[11] A. Ghimire, J. Song. ACS Appl. Mater. Interfaces, **13** (18), 20921–20937 (2021). DOI: 10.1021/acsami.1c01389
[12] V.E. Privalov, V.G. Shemanin, Izvestiya RAN. Seriya fizicheskaya, **79** (2), 170 (2015) (in Russian).
[13] O.V. Mkrtychev, V.E. Privalov, V.G. Shemanin, A.E. Fotiadi, Nauchno-Tekhicheskie Vedomosti SPbGPU. Fiziko-matematicheskie nauki, **1** (213) 128–135 (2015) (in Russian).
[14] V.E. Privalov, S.V. Polovchenko, P.V. Chartiy, Nauchno-Tekhicheskie Vedomosti SPbGPU. Fiziko-matematicheskie nauki, **4** (206), 64–73 (2014) (in Russian).
[15] P.E. Timchenko, E.V. Timchenko, L.T. Volova, M.A. Zybin, O.O. Frolov, G.G. Dolgushov. Opt. Mem. Neural Networks, **29** (4), 354–357 (2020). DOI: 10.3103/S1060992X20040116
[16] E.V. Timchenko, P.E. Timchenko, E.V. Pisareva, M.A. Daniel, L.T. Volova, A.A. Fedotov, O.O. Frolov, A.N. Subatovich. J. Optical Technology, **87** (3), 161–167 (2020). DOI: 10.1364/JOT.87.000161
[17] E.V. Timchenko, P.E. Timchenko, E.V. Pisareva, M.Yu. Vlasov, L.T. Volova, O.O. Frolov, Ya.V. Fedorova, G.P. Tikhomirova, D.A. Romanova, M.A. Daniel. Opt. Spectrosc., **128** (7), 989–997 (2020). DOI: 10.1134/S0030400X20070243

Translated by Y.Alekseev